35th Annual International Conference of the IEEE EMBS
Osaka, Japan, 3 - 7 July, 2013

Monitoring of temperature increase and tissue vaporization during laser interstitial thermotherapy of *ex vivo* swine liver by computed tomography

E. Schena, *Member, IEEE*, P. Saccomandi, *Student Member, IEEE*, F. Giurazza, R. Del Vescovo, L. Mortato, M. Martino, F. Panzera, F.M. Di Matteo, B. Beomonte Zobel, and S. Silvestri, *Member, IEEE*

Abstract— **Laser interstitial thermotherapy (LITT) is a minimally invasive technique used to thermally destroy tumour cells. Being based on hyperthermia, LITT outcome depends on the temperature distribution inside the tissue.**

Recently, CT scan thermometry, based on the dependence of the CT number (*HU*) on tissue temperature (*T*) has been introduced during LITT; it is an attractive approach to monitor T because it overcomes the concerns related to the invasiveness.

We performed LITT on nine *ex vivo* swine livers at three different laser powers, (P=1.5 W, P=3 W, P=5 W) with a constant treatment time t=200 s; *HU* is averaged on two ellipsoidal regions of interest (ROI) of 0.2 cm^2, placed at two distances from the applicator (d=3.6 mm and d=8.7 mm); a reference ROI was placed away from the applicator (d=30 mm).

The aim of this study is twofold: 1) to evaluate the effect of the T increase in terms of *HU* variation in *ex vivo* swine livers undergoing LITT; and 2) to estimate the P value for tissue vaporization. To the best of our knowledge, this is the first study focused on the *HU* variation in swine livers undergoing LITT at different P.

The reported findings could be useful to assess the effect of LITT on the liver in terms of both T changes and tissue vaporization, with the aim to obtain an effective therapy.

I. Introduction

Laser interstitial thermotherapy (LITT) is a minimally invasive technique used to destroy neoplastic masses in several organs, such as prostate, liver, lungs, brain [1] and, more recently, pancreas [2, 3]. The absorption of laser light, guided by an optical fiber inside the tumour to be treated, results in a localized heating, able to induce cellular death.

LITT outcome strongly depends on the temperature reached within the tissue during treatment, and the spatial temperature distribution defines the amount of vaporized and damaged volume. Therefore, the monitoring of temperature increase during the laser ablation is essential for effective therapy, in order to completely remove the neoplastic volume, and to avoid thermal damage of the surrounding healthy tissue.

Different systems have been used for monitoring the temperature during LITT: infrared external thermography, thermocouples [4], fluoroptic sensors, and Fiber Bragg Gratings (FBGs) sensors [5], among others. The main drawback of monitoring the external temperature is the extremely poor accuracy in the estimation of temperature inside the treated volumes. Whereas, monitoring temperature with thermocouples, fluoroptic and FBG sensors presents the major drawback of the invasivity. Furthermore, thermocouples and fluoroptic sensors introduce not-negligible insertion errors due to the direct absorption of laser light and self-heating [6]. On the other hand, FBGs require the use of expensive tools, such as an optical spectrum analyzer.

In order to overcome the abovementioned concerns, some studies focused the attention on the assessment of noninvasive thermometry based on medical imaging, i.e., MRI-, CT- and ultrasound-based thermometry. Recent improvements of CT scanner performances have encouraged investigations on feasibility of CT-based thermometry to provide a feedback in hyperthermia dosimetry.

This technique is based on the temperature-dependent change of *HU* in water and biological tissue samples that is known since the late 1970s [7]. However, at that time CT values were far from being stable, and reproducibility of quantitative CT measurements was not guaranteed. The recent improvements of the CT value stability in modern CT scanners have encouraged the development of some studies in this field [8].

The relationship between *HU* and *T* has been investigated for different media, such as water equivalent phantoms and 0.9% NaCl solution [9]. Recently, some researchers have applied this technique for temperature assessment during radiofrequency ablation of porcine livers [10, 11] and during LITT on bovine livers [12]; *HU* variation of porcine livers has also been assessed by heating the tissues with hot air flow [13].

The aims of the present research are: 1) to assess the *HU* decrease of *ex-vivo* swine livers undergoing LITT at three different P (i.e., 1.5 W, 3 W, 5 W) and at two distances, d, from the applicator (i.e., 3.6 mm, 8.7 mm) and 2) to assess the tissue vaporization during treatment.

This work has been carried out under the financial support of Filas-Regione Lazio in the framework of the ITINERIS2 project (CUP code F87G10000120009).

E. Schena, P. Saccomandi and S. Silvestri are with the Unit of Measurements and Biomedical Instrumentation, Center for Integrated Research, Università Campus Bio-Medico di Roma, Via Álvaro del Portillo, 21-00128- Rome-Italy.

F. M. Di Matteo, F. Panzera and M. Martino are with the GI Endoscopy Unit, Center for Integrated Research, University Hospital Campus Bio-Medico di Roma, Via Alvaro del Portillo, 21-00128- Rome-Italy.

F. Giurazza, R. Del Vescovo, L. Mortato and B.B. Zobel are with the Unit of Radiology, Università Campus Bio-Medico di Roma, Via Álvaro del Portillo, 200-00128-Rome-Italy.

II. Theoretical Background

Monitoring of T by CT scan images is based on the dependence of the *HU* on tissue density. The relationship between *HU* and *T* can be summarized by the following steps:

1) each pixel of a clinical image obtained by CT scan is represented by the *HU*, which is related to the attenuation properties of the tissue. The CT number is expressed as:

$$HU(x,y) = 1000\frac{\mu(x,y) - \mu_{H2O}}{\mu_{H2O}} \quad (1)$$

being μ_{H2O} the attenuation coefficient of water, and $\mu(x,y)$ the average attenuation coefficient of the tissue. The attenuation coefficient strongly depends on the tissue density, ρ, because the CT scan is performed with high energy x-rays. In this case the phenomenon of Compton scattering interactions, that mainly depends on ρ, causes the contrast;

2) under the hypothesis of linearity, ρ can be expressed as a function of temperature variation ΔT:

$$\rho(T) = \frac{\rho(T_0)}{1 + \alpha \cdot \Delta T} \quad (2)$$

where $\Delta T = T - T_0$, and T_0 is a reference temperature considered equal to the environmental one (i.e., 20 °C).

The dependence of the attenuation coefficient on *T* can be explained by considering (2) and the following relationship [14]:

$$\mu(T) = \left(\frac{\mu}{\rho}\right) \cdot \rho(T) \quad (3)$$

by definition the mass attenuation coefficient, μ/ρ, does not depend on ρ;

3) using the Taylor series linearization, the relationship between *HU* and *T* can be obtained by (1) and (2) as a function of the cubic thermal expansion coefficient, α:

$$HU(T) \approx HU(T_0) - 1000\frac{\mu(T_0) \cdot \alpha \cdot \Delta T}{\mu_{H2O}(T_0)} \quad (4)$$

$$\Delta HU(T) \approx -[1000 + HU(T_0)] \cdot \alpha \cdot \Delta T \quad (5)$$

where $\Delta HU(T) = HU(T) - HU(T_0)$ is the difference between *HU* at a generic *T* and *HU* at reference *T* (T_0).

Equation 5 shows a simplified relationship between ΔHU and *T*, which is valid under the simplifying hypothesis of linearity. The CT scan thermometry, used to monitor the temperature increase of a tissue undergoing LITT, is based on the above reported dependence (5); since during LITT the tissue temperature close to the applicator increases, *HU* will decrease, as predicted by (5).

III. Experimental Set Up and Methods

Nine *ex-vivo* swine livers were treated with a Nd:YAG laser (1064 nm, Smart 1064, DEKA M.E.L.A. s.r.l., Florence, Italy, Fig. 1A).

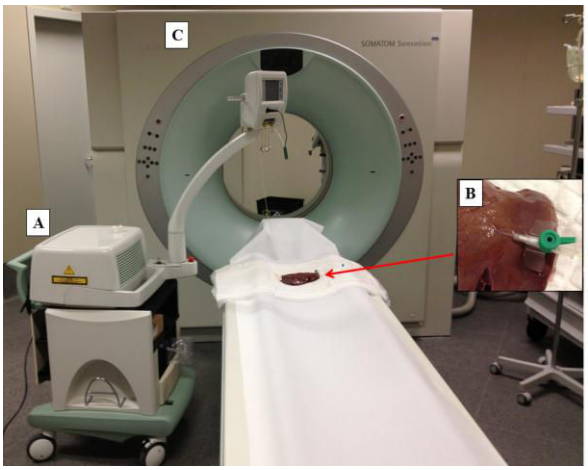

Figure 1. Experimental setup: A) laser source; B) laser applicator inside the *ex-vivo* liver; C) CT scanner.

The radiation was conveyed into a quartz bare fiber applicator with a core of 300 μm diameter (Fig. 1B) using the laser settings reported in Table I.

TABLE I. Laser Settings Used During LITT

Number of livers treated	P [W]	E [J]	t [s]
3	1.5	300	200
3	3	600	200
3	5	1000	200

During LITT, images were acquired by a CT scanner (Siemens Somatom 64 slices, Fig. 1C) at 150 mAs, 120 kVp and 0.6 mm slices. The total time required to scan the whole organ was 9 s; therefore this was the repetition time at which each slice was acquired. The averaged *HU* was calculated on two regions of interest (ROIs) with ellipsoidal shape of area=0.2 cm^2 and centered at d=8.7 mm (Fig. 2B) and d=3.6 mm (Fig. 2C) downward the applicator (Fig. 2A). A further ROI at a distance d=30 mm (Fig. 2D) from the applicator was used as reference.

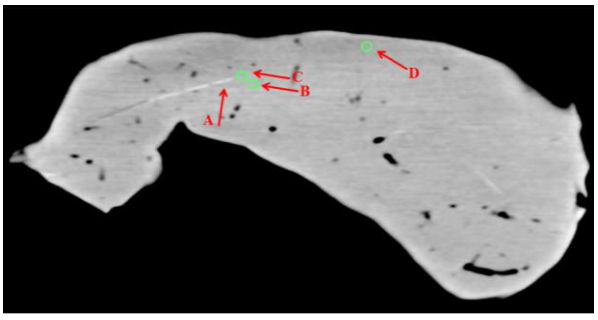

Figure 2. CT scan image of the liver: A) applicator; B) ROI at d=8.7 mm; C) ROI at d=3.6 mm of distance; D) ROI of reference (d=30 mm).

IV. Results and Discussion

All three livers undergoing LITT at P=1.5 W did not show vaporized region at the end of the treatment, as reported in Fig. 3B; on the other hand, all livers showed a vaporized region at the end of treatment when the laser power was 3 W and 5 W. This is depicted in Fig. 3D (P=3 W) and 3F (P=5 W) where the vaporized tissue are represented by hypodense regions. In both cases, the selected ROIs, surrounded by green circles, contain vaporized tissue at the end of treatment.

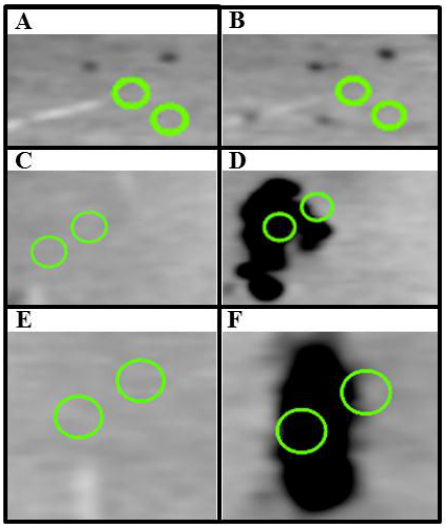

Figure 3. CT scan images of the liver close to the applicator. P=1.5 W: A) before and B) at the end of the treatment; P=3 W: C) before and D) at the end of the treatment; P=5 W: E) before and F) at the end of the treatment.

These results confirm data obtained in a previous work where LITT was carried out on *ex-vivo* pancreases [5]: at 1.5 W and same time of application the pancreases did not show a vaporized region; tissues showed vaporization when treated at 3 W, 6 W, and 10 W.

The averaged *HU* can be used to assess the presence of vaporized tissue because of its high variation when the liver tissue has undergone vaporization. In fact, at environmental temperature (22°C±2°C) the 9 *ex vivo* swine livers showed an averaged *HU* of about 77; this value agrees with the one reported in [9]. Experiments show that tissue vaporization causes a marked decreases of the *HU*: when a ROI contains only vaporized tissue (Fig. 3F), it shows an averaged *HU* lower than -450. The three livers treated at 3 W show a sudden decrease of the *HU* in the ROI closest to the applicator (d=3.6 mm) between 90 s and 99 s after the start of the treatment. At 5 W the vaporization starts earlier than at 3 W due to a steep increase of *T*; in fact the marked decrease of *HU* happens between 9 s and 18 s after the start of the treatment. These results agree with literature showing a higher and faster T increase when P increases [5, 15].

When the ROIs do not contain vaporized volume, the *HU* shows a slight decrease during treatment caused by the increase of *T*, as predicted by (4) and (5). This phenomenon can be used to observe the tissue temperature variation during LITT.

In order to assess the feasibility of monitoring temperature with CT-based thermometry during tissue hyperthermia induced by laser absorption, we calculated the ΔHU of the liver undergoing treatment as a function of time:

$$\Delta HU(t) = HU(t) - HU(T_0) \tag{6}$$

being $HU(T_0)$ the averaged *HU* in the selected ROI before the starting of treatment and $HU(t)$ the averaged *HU* in the selected ROI calculated after a treatment time *t*.

In Fig. 4 the trend of ΔHU during the treatment at P=1.5 W is shown for the two selected ROIs and the reference one. In the graphics are reported the mean of ΔHU calculated considering the three livers treated at 1.5 W.

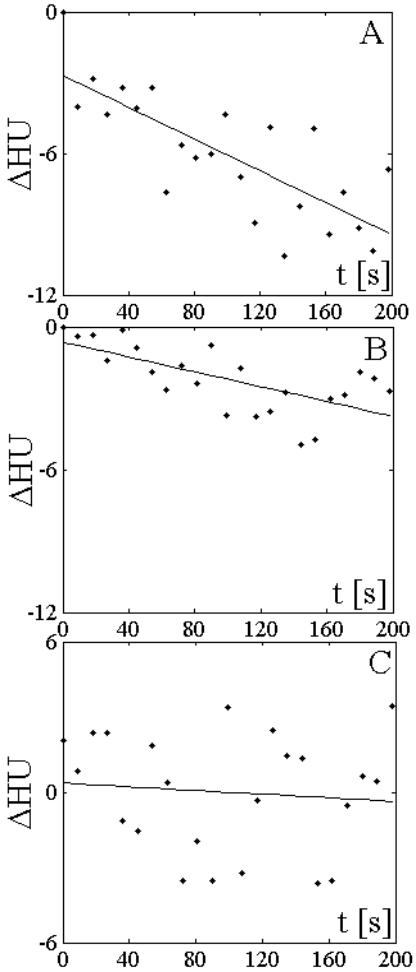

Figure 4. Averaged ΔHU *vs t* during the treatment at P=1.5 W in the ROI at the three distances: A) d=3.6 mm; B) d=8.7 mm; C) d=30 mm. The best fitting lines are also reported.

As it is well-known [1], the shorter the distance from the applicator, the higher the temperature increase of tissue having undergone LITT. Therefore, taking into account (5), we expected a more marked decrease of ΔHU within the ROI close to the applicator (d=3.6mm) than in the ROI at 8.7 mm. This is confirmed by experimental data, by comparing Fig. 4A with Fig. 4B; furthermore, this result is strengthened considering a simple linear relationship between ΔHU and *t*: 1) in both mentioned ROIs the averaged *HU* decreases during treatment due to the increase of *T*; 2) in the ROI placed at 3.6 mm (Fig. 4A) the decrease of *HU* is more evident than in the ROI placed at 8.7 mm (Fig. 4B). This

result is confirmed by the slope of the best fitting lines reported in Table II; 3) In the ROI used as reference (d=30 mm), the tissue did not show any significant temperature increase during treatment; this is also confirmed by the flat trend of the *ΔHU* (Fig. 4C) showing a negligible slope (-0.004 s^{-1}).

TABLE II. LINEAR REGRESSION BETWEEN Δ*HU* OF THE THREE ROIS AND TIME AT P=1.5 W. SLOPE, CORRELATION COEFFICIENT AND SINGIFICATIVITY OF THE BEST FITTING LINE ARE REPORTED

d	P [W]	slope [s^{-1}]	R^2	ρ
3.6 mm	1.5	-0.034	0.60	<0.001
8.7 mm	1.5	-0.016	0.46	<0.001
30 mm	1.5	-0.004	0.009	No sign

Only at high distance (i.e., 30 mm) *HU* results almost constant during the treatment and Δ*HU* and *t* are not significantly correlated.

V. CONCLUSION

To the best of our knowledge, this is the first study focused on the *ΔHU* variation of swine liver undergoing LITT at different P. Vaporized region was not present in liver treated at 1.5 W, whereas it was evident in livers treated at 3 W and 5 W; these results agree with the ones reported in a previous study on porcine pancreases [5].

During LITT, the relative distance between the selected ROIs and the applicator, strongly influences the *HU* decrease; in fact, a smaller *HU* decrease is associated with a greater distance from the applicator, and it is negligible at 30 mm because *T* is almost constant [5, 16].

These findings show that *HU* variation can be used to assess the tissue region interested to a consistent T increase during treatment.

In conclusion, the assessment of the *HU* variation could be useful to monitor the effects of LITT in terms of both *T* variation and the presence of vaporized tissue, with the aim to obtain an effective therapy. The introduction of CT based thermometry in this field is also encouraged by some advantages, such as the non-invasivity and the chance to track tissue modifications during the procedure.

REFERENCES

[1] G. Müller and A. Roggan, "Laser-Induced Interstitial Thermotherapy", 1st ed., Washington USA: SPIE Optical Engineering Press, 1995, pp. 375-506.

[2] P. Saccomandi *et al.*, "Laser Interstitial Thermotherapy for pancreatic tumor ablation: theoretical model and experimental validation," in *Proc. 33rd Annu. International Conf. IEEE Eng. Med. Biol. Soc.*, Boston, 2011, pp. 5585-5588.

[3] P. Saccomandi *et al*., "Theoretical assessment of principal factors influencing laser interstitial thermotherapy outcomes on pancreas," in Proc. 34th Annu. International Conf. IEEE Eng. Med. Biol. Soc., San Diego, 2012, pp. 5687-5690.

[4] F. Manns, P. J. Milne, X. Gonzalez-Cirre, D. B. Denham, J. M. Parel and D. S. Robinson, "In Situ Temperature Measurement With Thermocouple Probes During Laser Interstitial Thermotherapy (LITT): Quantification and Correction of a Measurement" *Artifact Laser Surg. Med*., vol. 23, pp. 94-103, 1998.

[5] P. Saccomandi, E. Schena, M. A. Caponero, F. M. Di Matteo, M. Martino, M. Pandolfi and S. Silvestri, "Theoretical Analysis and Experimental Evaluation of Laser-Induced Interstitial Thermotherapy in Ex Vivo Porcine Pancreas," *IEEE T Bio-Med Eng*, vol. 59, pp. 2958-64, 2012.

[6] A. D. Reid, M. R. Gernet and M. D. Sherar, "Temperature measurement artefacts of thermocouples and fluoroptic sensor during laser irradiation at 810 nm," *Phys. Med. Biol.*, vol. 46, pp. N149-N157, 2001.

[7] G. M. Bydder, L. Kreel, "The temperature dependence of computed tomography attenuation values," *J. Comput. Assist. Tomogr.,* vol. 3, pp. 506-510, 1979.

[8] A. H. Mahnken, P. Bruners, "CT thermometry: will it ever become ready for use?," *Int. J. Clin. Pract*., vol. 65, pp. 1-2, 2011.

[9] P. Bruners *et al.* "Multi-slice computed tomography: A tool for non-invasive temperature measurements?," *Int. J. Hyperther*., vol. 26, pp. 359-365, 2010.

[10] P. Bruners *et al.* "CT-based temperature monitoring during hepatic RF ablation: Feasibility in an animal model," *Int. J. Hyperther*., vol. 28, pp. 55-61, 2012.

[11] G. D. Pandeya, M. G. V. Greuter, B. Schimdt, T. Flohr and M. Oudkerk, "Assessment of thermal sensitivity of CT during heating of liver: an ex vivo study," *Brit. J. Radiol.*, vol. 85, pp. e661-e665, 2012.

[12] G. D. Pandeya, M. G. V. Greuter, K. P. De Jong, B. Schimdt, T. Flohr and M. Oudkerk, "Feasibility of computed tomography based thermometry during interstitial laser heating in bovine liver," *Eur. Radiol.*, vol. 21, pp. 1733-1738, 2011.

[13] G. D. Pandeya, M. J. W. Greuter, K. P. De Jong, B. Schmidt, T. Flohr and M. Oudkerk, "Feasibility of noninvasive temperature assessment during radiofrequency liver ablation on computed tomography," *J. Comput. Assist. Tomogr.*, vol. 35, pp. 356-360, 2011.

[14] P. Homolka, A. Gahleitner and R. Nowotny, "Temperature dependence of HU values for various water equivalent phantom materials," *Phys. Med. Biol.*, vol. 47, pp. 2917-2923, 2002.

[15] S. C. Jiang and X. X. Zhang, "Dynamic modeling of photothermal interactions for laser induced interstitial thermotherapy: parameter sensitivity analysis," *Lasers Med. Sci.*, vol. 20, pp. 122-131, 2005.

[16] B. M. Lippert, A. Teymoortash, B. J. Folz and J. A. Werner, "Coagulation and temperature distribution in Nd:YAG interstitial laser thermotherapy: an in vivo animal study," *Lasers Med. Sci.*, vol. 18, pp. 19-24, 2003.